Advanced Powder Technology xxx (2013) xxx–xxx

Contents lists available at SciVerse ScienceDirect

Advanced Powder Technology

journal homepage: www.elsevier.com/locate/apt

Original Research Paper

In situ fabrication of carbon nanotube–$MgAl_2O_4$ nanocomposite powders through hydrogen-free CCVD

Mehran Bolourian Kashi [a,*], Roya Aghababazadeh [b], Hossein Arabi [c], Alireza Mirhabibi [d]

[a] School of Metallurgy and Materials Engineering, Iran University of Science and Technology (IUST), Narmak, Tehran, Iran
[b] Institute for Color Science and Technology (ICST), Lavizan, Tehran, Iran
[c] Center of Excellence for High Strength Alloys Technology (CEHSAT), Iran University of Science and Technology, Narmak, Tehran, Iran
[d] Center of Excellence for Ceramic Materials in Energy and Environment Applications, Iran University of Science and Technology, Narmak, Tehran, Iran

ARTICLE INFO

Article history:
Received 3 October 2012
Received in revised form 9 April 2013
Accepted 11 April 2013
Available online xxxx

Keywords:
Carbon nanotubes
Catalytic chemical vapor deposition (CCVD)
Raman spectroscopy and scattering
Electron microscopy
Oxides

ABSTRACT

Carbon nanotube–$MgAl_2O_4$ composite powders were successfully prepared through solution combustion synthesis (SCS) followed by catalytic chemical vapor deposition (CCVD) of methane. Catalyst powders were synthesized starting with the stoichiometric ratios of metal nitrates and urea with a small amount of water and different Fe contents followed by subjecting the solution to heat. The obtained powders were placed in a silica tube to react with methane and form carbon nanotubes. It is noteworthy that no hydrogen was used throughout the whole process. Catalysts and composite powders were characterized by X-ray diffraction (XRD), scanning electron microscopy (SEM), transmission electron microscopy (TEM) and Raman spectroscopy. The quality of products were evaluated by I_D/I_G ratio obtained from G and D bands intensities in Raman spectra of samples having 10 and 15 wt.% iron. The final product mostly comprised a mixture of single- and double-walled nanotubes on the catalyst containing 10 wt.% Fe, while no carbon product was formed on the catalyst with 5 wt.% Fe.

© 2013 The Society of Powder Technology Japan. Published by Elsevier B.V. and The Society of Powder Technology Japan. All rights reserved.

1. Introduction

After Iijima's report of carbon nanotubes (CNTs) [1], owing to unique properties and application of these structures [2–7], significant efforts have been dedicated to find new and suitable routes of synthesizing them. There are three major processes of producing CNTs: arc discharge, laser ablation and catalytic chemical vapor deposition (CCVD). Among these, CCVD has several advantages over the other two: the mild conditions in this process allow more control over the growth step and more importantly, CCVD is the most amenable method for scale-up purposes [8,9]. In this method, presence of a catalyst material is inevitable and catalyst and catalyst support materials as well as their interaction are of great importance for the type and quality of CNT products. Among various catalyst preparation routes [10–12], solution combustion synthesis (SCS) is a promising way to achieve a homogenous and fine powder with high surface area which enables producing high-tech oxides and solid solutions [13–15] that makes it a suitable method of catalyst preparation for CNT synthesis by CCVD [16–19].

In addition to the catalyst, the gasses used in the growth step of the CCVD process are of great importance, since they are integral to achieve the desired product with optimum properties. Among them, hydrogen is a widely used gas which controls the final product by acting as a reducing agent and by controlling the thermodynamics of the hydrocarbon cracking reaction as well. However, in some cases, use of hydrogen was reported to be detrimental to the final CNT yield and quality (according to I_D/I_G ratio obtained from the Raman spectra) [20,21]. Moreover, several high resolution transmission electron microscope (HRTEM) images are reported in the literature which employed a mixture of H_2 and CH_4, showing the formation of large (>5 nm) iron nanoparticles covered with graphene layers which as a consequence, make the catalyst nanoparticles inactive for CNT nucleation and growth [22–24].

Hydrogen-free synthesis of CNTs over Fe/Al_2O_3, Fe/SiO_2 [25–26] and Fe/MgO [27] are reported previously. However, among the surveyed literature, growth of CNTs over $Fe/MgAl_2O_4$ was always performed using a mixture of H_2 and CH_4 [17,28,29]. Therefore, one may think that the use of hydrogen is indispensible in order to synthesize CNTs on $Fe/MgAl_2O_4$ catalysts.

Here we report preparation of $Fe/MgAl_2O_4$ catalysts through SCS, followed by successful H_2-free CCVD at 900 °C in order to obtain CNTs, only using the reduction ability of CH_4.

2. Materials and methods

2.1. Synthesis of catalyst powders

Three catalyst powders were synthesized starting with stoichiometric mixture of metal nitrates and urea according to [14],

* Corresponding author. Tel.: +98 21 77240540x2811; fax: +98 21 77240480.
E-mail address: m.bolourian.k@gmail.com (M. Bolourian Kashi).

0921-8831/$ - see front matter © 2013 The Society of Powder Technology Japan. Published by Elsevier B.V. and The Society of Powder Technology Japan. All rights reserved.
http://dx.doi.org/10.1016/j.apt.2013.04.007

Please cite this article in press as: M. Bolourian Kashi et al., *In situ* fabrication of carbon nanotube–$MgAl_2O_4$ nanocomposite powders through hydrogen-free CCVD, Advanced Powder Technology (2013), http://dx.doi.org/10.1016/j.apt.2013.04.007

Fig. 1. Catalyst foam before grinding by agate mortar, obtained after the combustion process.

therefore the equivalence ratio, Φ_e, equals unity. Specific amounts of aluminum nitrate ($Al(NO_3)_3{\cdot}9H_2O$, Merck), magnesium nitrate ($Mg(NO_3)_2{\cdot}6H_2O$, Merck) and urea (CH_4N_2O, Merck) were mixed along with desired amount of iron nitrate ($Fe(NO_3)_3{\cdot}9H_2O$ Merck) and minimum amount of deionized water (3 mL). Magnesium nitrate to aluminum nitrate ratio were adjusted to obtain exactly 1 g of $MgAl_2O_4$ spinel and iron nitrate was added to achieve 5, 10 and 15 wt.% $Fe/MgAl_2O_4$ ratios. The resulting mixture was heated and stirred on a heater-stirrer to obtain a clear orange solution. The Pyrex vessel was then placed in a preheated muffle furnace (500 °C), until the reaction took place. The fluffy products were ground and designated FAM5, FAM10 and FAM15 for the iron content of 5, 10 and 15 wt.% iron, respectively.

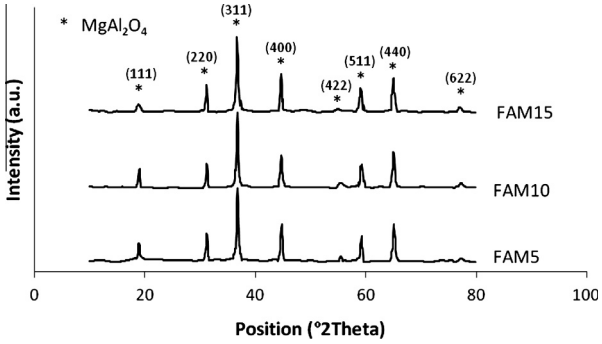

Fig. 2. XRD patterns of catalyst powders (5, 10 and 15 wt.% Fe).

2.2. Growth of CNTs

Catalyst powder (0.1 g) was put in an alumina boat. The boat was placed in a silica tube, mounted in a horizontal tube furnace. Temperature was raised to 900 °C under N_2 (99.99% purity) atmosphere with the rate of 15.5 °C/min and N_2 flow of 350 cm^3/min. Afterwards, N_2 was switched to methane (99.995% purity, TGS) for 5 min with the flow rate of 6000 cm^3/min. As soon as the reaction time finished, methane was switched back to N_2 and the specimen was cooled down to room temperature. The resulting powders were designated NTFAM5, NTFAM10 and NTFAM15 for the catalysts with 5, 10 and 15 wt.% Fe, respectively.

2.3. Characterization of catalysts and products

Catalyst powders were analyzed by X-ray diffraction (XRD) using JEOL X-ray diffractometer with Cu Kα. Scanning electron

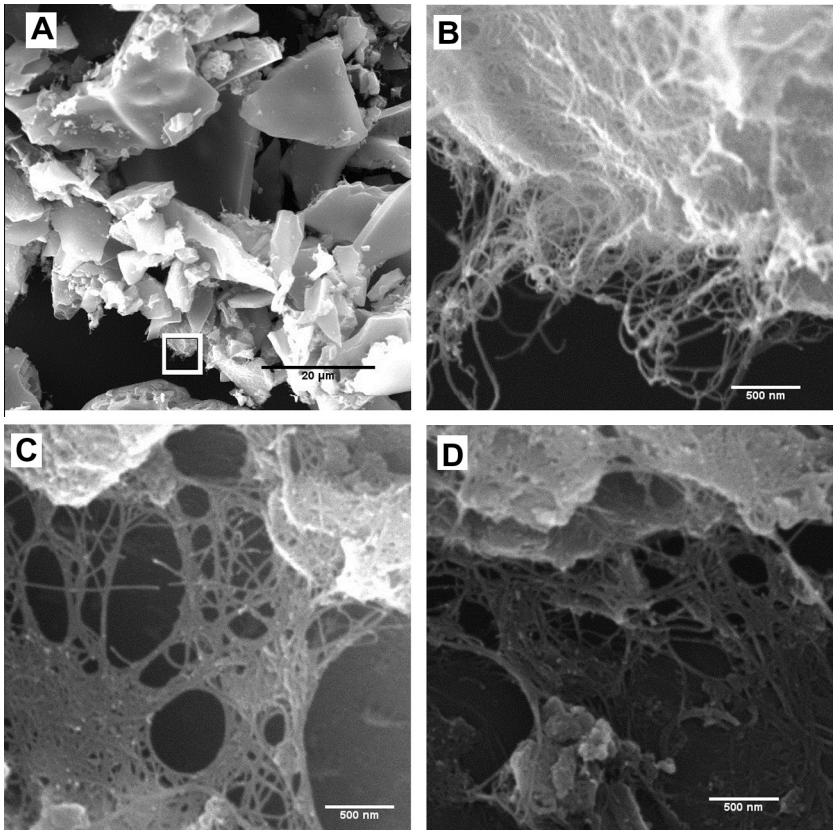

Fig. 3. SEM micrographs of CNTs grown on (A) and (B) FAM10, and (C) and (D) FAM15 catalysts. Image (B) is higher magnification of the white square in (A).

Please cite this article in press as: M. Bolourian Kashi et al., *In situ* fabrication of carbon nanotube–$MgAl_2O_4$ nanocomposite powders through hydrogen-free CCVD, Advanced Powder Technology (2013), http://dx.doi.org/10.1016/j.apt.2013.04.007

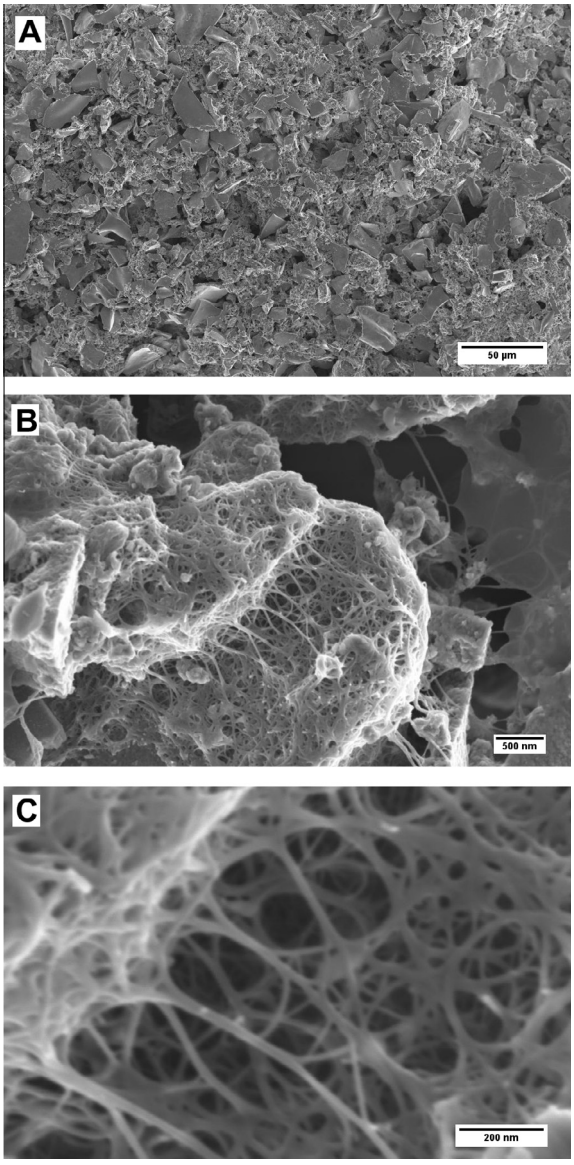

Fig. 4. FEGSEM micrographs of CNTs grown on FAM10 catalyst.

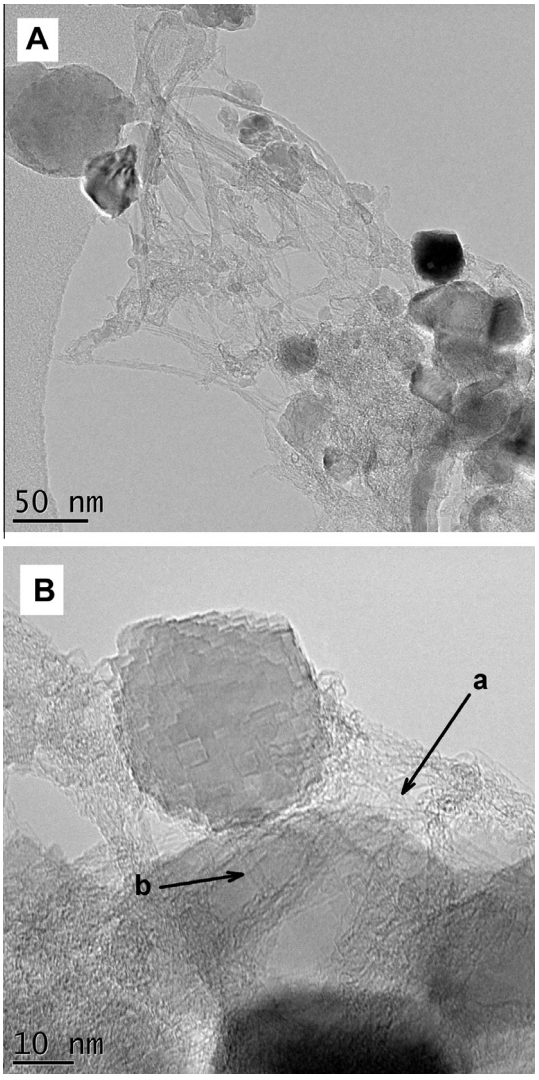

Fig. 5. TEM images of NTFAM10. *a* indicates a SWNT with the diameter of 1.8 nm and *b* shows a DWNT with inner and outer diameter of 1.2 and 2.2 nm, respectively.

microscopy (SEM) micrographs were obtained by a Wega II Tescan and LEO1530 FEGSEM microscope. TEM images were obtained by a Philips CM200-FEG microscope. Specimens were prepared as follows: A small amount of as-synthesized CNTs were dispersed in acetone followed by sonication. A droplet of the suspension was poured on a glass piece for SEM or on a copper grid for TEM and let dry. Micro-Raman spectra were obtained using an Almega Thermo Nicolet Dispersive Raman Spectrometer with second harmonic Nd:YLF laser at 532 nm. I_D/I_G ratios were calculated by dividing the area under D band by G band peaks using Lorentzian peak fitting in Origin software.

3. Results and discussion

After placing the solution in the preheated muffle furnace, it started boiling immediately. The water evaporated and the solution frothed and ignited with a blazing flame and a linear reaction took place. The whole process was completed in less than 5 min. The color of the resulting powder was pale green for the catalyst with 5 wt.% Fe, green for 10 wt.% and green with smattering brown for 15 wt.% Fe. Worth mentioning, the green color is representative of Fe^{2+} and red corresponds to Fe^{3+} ions [16]. The FAM15 foam obtained after the combustion reaction is shown in Fig. 1. Fig. 2 illustrates XRD patterns of the three catalyst powders after SCS process. The patterns clearly confirm the formation of spinel phase for all three samples, while no evidence of iron species peaks is found. Therefore, it is concluded that all the iron species are dissolved into the spinel lattice, forming an oxide solid solution. Crystallite size of the three catalyst powders were measured as the average of crystallite sizes obtained from (311), (400), and (440) peaks according to Scherrer method (Eq. (1)) [30]:

$$d = \frac{K\lambda}{\beta \cos\theta} \tag{1}$$

where d is the mean crystallite size, K is the shape factor which for near spherical crystallites equals 0.9, λ is the X-ray wavelength, β is the integral breadth (area/amplitude), and θ is the Bragg angle. The calculated values are 19, 23, and 45 nm for FAM5, FAM10, and FAM15, respectively. One can see that the crystallite size increases with iron content. Though, the increase from 10 to 15 wt.% iron is much more significant than the increase from 5 to 10 wt.% iron. A possible explanation is the presence of more vacancies in FAM15 catalyst powder. In $MgAl_2O_4$ spinel, Mg ions occupy tetrahedral

Please cite this article in press as: M. Bolourian Kashi et al., *In situ* fabrication of carbon nanotube–$MgAl_2O_4$ nanocomposite powders through hydrogen-free CCVD, Advanced Powder Technology (2013), http://dx.doi.org/10.1016/j.apt.2013.04.007

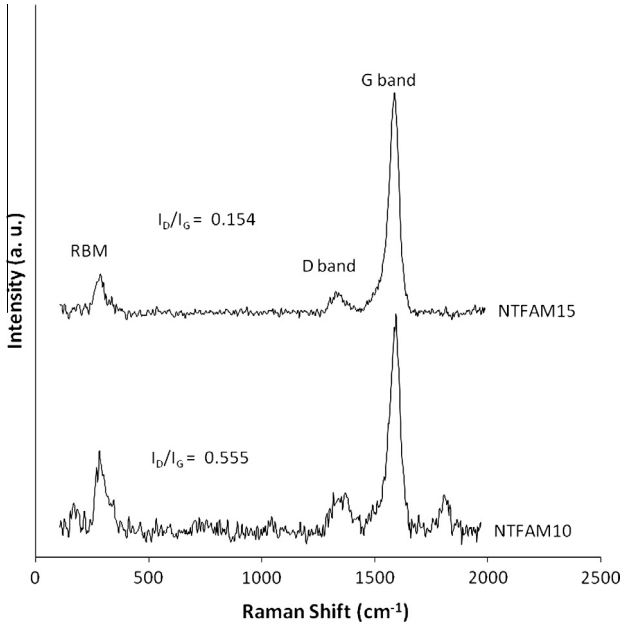

Fig. 6. Raman spectra of NTFAM10 and NTFAM15.

Table 1
Summary of the catalysts and products properties.

Catalyst	Iron content (wt.%)	Color	Crystallite size (nm)	CNTs	I_D/I_G
FAM5	5	Pale green	19	No	–
FAM10	10	Green	23	Yes	0.555
FAM15	15	Green and brown	45	Yes	0.145

sites and Al ions occupy octahedral sites. As the XRD patterns in Fig. 2A confirmed the formation of a solid solution, several ion substitution states are possible: Fe^{2+} for Mg^{2+}, Fe^{3+} for Al^{3+}, Fe^{2+} for Al^{3+}, and Fe^{3+} for Mg^{2+}. The last two states lead to formation of vacancies: three Mg^{2+} ions replace with two Fe^{3+} ions and one Mg^{2+} vacancy (Eq. (2)), or two Al^{3+} ions replace with two Fe^{2+} ions and one oxygen vacancy (Eq. (3)):

$$3Mg_{Mg}^{2+} \rightleftharpoons 2Fe_{Mg}^{3+} + V''_{Mg} \quad (2)$$

$$2Al_{Al}^{3+} \rightleftharpoons 2Fe_{Al}^{2+} + V_0^{\cdot\cdot} \quad (3)$$

Presence of vacancies facilitates the ion migration and thermal diffusion. Due to higher iron content, it is anticipated that the amount of these vacancies is much higher in FAM15 than in the other two catalysts. As a result, at high temperatures, coarsening of the crystallites occurs throughout the combustion process which leads to higher crystallite size of FAM15 powder.

Fig. 3 shows SEM micrographs of the CNTs grown on the catalysts. It is interesting to note that no CNTs were found on FAM5 catalyst powder. Since CNTs were formed on catalysts with higher iron content, it shows that the low iron content in FAM5 was not enough to provide CNT nucleation and growth sites on the surface of $MgAl_2O_4$ support. In Fig. 3A, large particles of FAM10 catalyst powder can be seen. Sharp edges show that these particles were fractured from larger particles through grinding the foam by the agate mortar after the combustion process. Fig. 3B is a higher magnification image of NTFAM10 and Fig. 3C and D shows micrographs of CNTs on FAM10 catalyst. A comparison between Fig. 3B–D reveals that the CNTs on FAM10 catalyst are thinner than those on FAM15 which indicates that the CNTs on FAM10 catalyst have fewer walls.

Fig. 4A is a low magnification FEGSEM micrograph of CNTs grown on FAM10. In Fig. 4B, bundles of CNTs can be seen which have bridged between catalyst particles. Fig. 4C shows higher magnification of NTFAM10 specimen in which branching of many CNT bundles has occurred. Formation of bundles and branching of them is a characteristic of few-walled (single, double, or triple) CNTs.

TEM images of NTFAM10 are shown in Fig. 5. According to these images, the main product on this catalyst is a mixture of SWNTs and DWNTs. Although it is not possible to count the number of walls in Fig. 5A, the low diameter of the tubes in Fig. 5B (between 1.8 and 2.2) relates to single and double-walled CNTs. Moreover, further studies by Raman spectroscopy revealed the presence of RBM peaks in the spectra of both specimens which are direct evidence for the presence of SWNTs and DWNTs. In Fig. 5A, catalyst particles and nanotubes surrounding them can be seen. In Fig. 5B, point *a* shows a SWNT 1.8 nm thick and point *b* indicates a DWNT with inner and outer diameter of 1.2 and 2.2 nm, respectively.

Raman spectra of NTFAM10 and NTFAM15 are illustrated in Fig. 6. The corresponding I_D/I_G ratio of each sample is calculated and brought above the spectrum. The I_D/I_G ratio obtained from D and G bands intensities in Raman spectra is a characteristic of nanotubes quality. G band appears at ~1590, D appears at ~1340 and radial breathing mode (RBM) below 400 cm^{-1}. Increase in I_D/I_G factor shows lower quality and presence of more defects in the products [31]. Therefore, it seems that higher iron content in FAM15 leads to more suitable sites for nanotube nucleation and growth that absorbs the carbon produced from methane dissociation and converts it into crystalline carbon nanotubes on catalyst particles. In the case of FAM10 catalyst, it is anticipated that presence of lower suitable nucleation sites lead to accumulation of carbon atoms around a catalyst particle and as a result, caused a higher amount of defective carbon and I_D/I_G ratio. Table 1 summarizes the catalysts and the products properties.

4. Conclusions

$Fe/MgAl_2O_4$ catalysts were prepared through solution combustion synthesis and carbon nanotube–$MgAl_2O_4$ nanocomposite powders were successfully fabricated by *in situ* H_2 free-CCVD.

X-ray diffraction patterns of the catalysts after the combustion reaction confirmed the formation of an oxide solid solution in which only spinel peaks appeared for the three catalysts and no evidence of iron peaks was found.

Results demonstrated that the iron content plays an integral role in hydrogen-free CCVD of CNTs in a way that no nanotubes were formed on the catalyst with 5 wt.% Fe. Moreover, quality of the products on the 15 wt.% Fe catalyst was higher than that of the nanotubes grown on 10 wt.% Fe catalyst as obtained from the Raman spectra. The product on the 10 wt.% Fe catalyst, as TEM images revealed, was a mixture of SWNTs and DWNTs.

Acknowledgments

One of the authors would like to thank Prof. Barros and the authors would like to thank University of Leeds LEMAS for technical support.

References

[1] S. Iijima, Helical microtubules of graphitic carbon, Nature 354 (1991) 56–58.
[2] Y. Li, J. Zhu, S. Wei, J. Ryu, Q. Wang, L. Sun, Z. Guo, Poly(propylene) nanocomposites containing various carbon nanostructures, Macromol. Chem. Phys. 212 (2011) 2429–2438.
[3] J. Zhu, M. Chen, N. Yerra, N. Haldolaarachchige, S. Pallavkar, Z. Luo, T.C. Ho, J. Hopper, D.P. Young, S. Wei, Z. Guo, Microwave synthesized magnetic tubular

carbon nanocomposite fabrics toward electrochemical energy storage, Nanoscale 5 (2013) 1825–1830.
[4] H. Gu, S. Tadakamalla, X. Zhang, Y. Huang, Y. Jiang, H.A. Colorado, Z. Luo, S. Wei, Z. Guo, Epoxy resin nanosuspensions and reinforced nanocomposites from polyaniline stabilized multi-walled carbon nanotubes, J. Mater. Chem. C 1 (2013) 729–743.
[5] H. Gu, S.B. Rapole, Y. Huang, D. Cao, Z. Luo, S. Wei, Z. Guo, Synergistic interactions between multi-walled carbon nanotubes and toxic hexavalent chromium, J. Mater. Chem. A 1 (2013) 2011–2021.
[6] J. Zhu, H. Gu, Z. Luo, N. Haldolaarachige, D.P. Young, S. Wei, Z. Guo, Carbon nanostructure-derived polyaniline metacomposites: electrical, dielectric, and giant magnetoresistive properties, Langmuir 28 (2012) 10246–10255 (2012/07/10).
[7] J. Zhu, S. Pallavkar, M. Chen, N. Yerra, Z. Luo, H.A. Colorado, H. Lin, N. Haldolaarachchige, A. Khasanov, T.C. Ho, D.P. Young, S. Wei, Z. Guo, Magnetic carbon nanostructures: microwave energy-assisted pyrolysis vs. conventional pyrolysis, Chem. Commun. (Cambridge, United Kingdom) 49 (2013) 258–260.
[8] P.J.F. Harris, Carbon Nanotube Science: Synthesis, Properties and Applications, Cambridge University Press, 2010.
[9] M.S. Dresselhaus, G. Dresselhaus, P.C. Eklund, Science of Fullerenes and Carbon Nanotubes, Elsevier Science, 1996.
[10] E. Lamouroux, P. Serp, P. Kalck, Catalytic routes towards single wall carbon nanotubes, Cat. Rev. 49 (2007) 341–405.
[11] Q. Wang, H.H. Tay, Z. Guo, L. Chen, Y. Liu, J. Chang, Z. Zhong, J. Luo, A. Borgna, Morphology and composition controllable synthesis of Mg–Al–CO_3 hydrotalcites by tuning the synthesis pH and the CO_2 capture capacity, Appl. Clay Sci. 55 (2012) 18–26.
[12] Q. Wang, Y. Gao, J. Luo, Z. Zhong, A. Borgna, Z. Guo, D. O'Hare, Synthesis of nano-sized spherical Mg_3Al–CO_3 layered double hydroxide as a high-temperature CO_2 adsorbent, RSC Adv. 3 (2013) 3414–3420.
[13] K.C. Patil, Advanced ceramics: combustion synthesis and properties, Bull. Mater. Sci. 6 (1993) 533–541.
[14] K.C. Patil, M.S. Hedge, T. Rattan, S.T. Aruna, Chemistry of Nanocrystalline Oxide Materials: Combustion Synthesis, Properties and Applications, World Scientific Publishing, 2008.
[15] C.-C. Hwang, T.-Y. Wu, J. Wan, J.-S. Tsai, Development of a novel combustion synthesis method for synthesizing of ceramic oxide powders, Mater. Sci. Eng., B 111 (2004) 49–56.
[16] P. Coquay, E. De Grave, A. Peigney, R.E. Vandenberghe, C. Laurent, Carbon nanotubes by a CVD method. Part I: synthesis and characterization of the (Mg,Fe)O catalysts, J. Phys. Chem. B 106 (2002) 13186–13198.
[17] E. Flahaut, A. Govindaraj, A. Peigney, C. Laurent, A. Rousset, C.N.R. Rao, Synthesis of single-walled carbon nanotubes using binary (Fe, Co., Ni) alloy nanoparticles prepared in situ by the reduction of oxide solid solutions, Chem. Phys. Lett. 300 (1999) 236–242.
[18] E. Flahaut, A. Peigney, C. Laurent, A. Rousset, Synthesis of single-walled carbon nanotube–Co–MgO composite powders and extraction of the nanotubes, J. Mater. Chem. 10 (2000) 249–252.
[19] P. Landois, A. Peigney, C. Laurent, L. Frin, L. Datas, E. Flahaut, CCVD synthesis of carbon nanotubes with W/Co–MgO catalysts, Carbon 47 (2009) 789–794.
[20] H. Ago, K. Nakamura, N. Uehara, M. Tsuji, Roles of metal-support interaction in growth of single- and double-walled carbon nanotubes studied with diameter-controlled iron particles supported on MgO, J. Phys. Chem. B 108 (2004) 18908–18915.
[21] G. Ning, F. Wei, Q. Wen, G. Luo, Y. Wang, Y. Jin, Improvement of Fe/MgO catalysts by calcination for the growth of single- and double-walled carbon nanotubes, J. Phys. Chem. B 110 (2005) 1201–1205.
[22] A. Peigney, C. Laurent, A. Rousset, Influence of the composition of a H_2–CH_4 gas mixture on the catalytic synthesis of carbon nanotubes-Fe/Fe_3C–Al_2O_3 nanocomposite powders, J. Mater. Chem. 9 (1999) 1167–1177.
[23] V.G. de Resende, E. De Grave, A. Cordier, A. Weibel, A. Peigney, C. Laurent, Catalytic chemical vapor deposition synthesis of single- and double-walled carbon nanotubes from α-$(Al_{1-x}Fe_x)2O_3$ powders and self-supported foams, Carbon 47 (2009) 482–492.
[24] A. Cordier, V.G.d. Resende, E.D. Grave, A. Peigney, C. Laurent, CCVD synthesis of single- and double-walled carbon nanotubes: influence of the addition of molybdenum to Fe–Al_2O_3 self-supported foams, J. Phys. Chem. C 112 (2008) 18825–18831 (2008/12/04).
[25] A.M. Cassell, J.A. Raymakers, J. Kong, H. Dai, Large scale CVD synthesis of single-walled carbon nanotubes, J. Phys. Chem. B 103 (1999) 6484–6492.
[26] J. Kong, A.M. Cassell, H. Dai, Chemical vapor deposition of methane for single-walled carbon nanotubes, Chem. Phys. Lett. 292 (1998) 567–574.
[27] H. Ago, N. Uehara, N. Yoshihara, M. Tsuji, M. Yumura, N. Tomonaga, T. Setoguchi, Gas analysis of the CVD process for high yield growth of carbon nanotubes over metal-supported catalysts, Carbon 44 (2006) 2912–2918.
[28] A. Govindaraj, E. Flahaut, C. Laurent, A. Peigney, A. Rousset, C.N.R. Rao, An investigation of carbon nanotubes obtained from the decomposition of methane over reduced Mg1–xM$x$$Al_2O_4$ spinel catalysts, J. Mater. Res. 14 (1999) 2568–2576.
[29] P. Coquay, E. De Grave, R.E. Vandenberghe, C. Dauwe, E. Flahaut, C. Laurent, A. Peigney, A. Rousset, Mössbauer spectroscopy study of $MgAl_2O_4$-matrix nanocomposite powders containing carbon nanotubes and iron-based nanoparticles, Acta Mater. 48 (2000) 3015–3023.
[30] B.D. Cullity, Elements of X-Ray Diffraction, Addison-Wesley, 1956.
[31] J.C. Charlier, Defects in carbon nanotubes, Acc. Chem. Res. 35 (2002) 1063–1069.

Please cite this article in press as: M. Bolourian Kashi et al., *In situ* fabrication of carbon nanotube–$MgAl_2O_4$ nanocomposite powders through hydrogen-free CCVD, Advanced Powder Technology (2013), http://dx.doi.org/10.1016/j.apt.2013.04.007